SSC00-III-5

Thermal Reflector System Design and Testing for the Microwave Anisotropy Probe

Hans D. Neubert[1], Wayne Chen[2]

[1]Programmed Composites, Inc., Corona, CA
[2]NASA/Goddard Space Flight Center, Greenbelt, MD

Abstract

Scheduled for a June 2001 launch, the Microwave Anisotropy Probe's (MAP) mission is to study in detail the cosmic microwave background radiation temperature fluctuations of the universe. The cosmic microwave background is the remnant afterglow of the Big Bang, and the tiny temperature differences from place to place on the sky provides a wealth of information about the basic nature of our universe. The observatory consists of dual back-to-back Gregorian optics and dual differential pseudo-correlation microwave radiometers. MAP will scan the sky over a 22 to 90 Ghz spectrum during a 26 month mission at L2. To achieve the necessary dimensional stability and stringent total weight limits, the Thermal Reflector System (TRS) consists of dual primary and secondary lightweight composite reflectors mounted to a lightweight but rigid composite truss structure. Design features include the use of lightweight graphite spread fabric and honeycomb core for the reflector shells and stiffening structure, and a bonded mortise and tenon truss structure using two complementary composite materials. Qualification of the TRS included in-situ photogrammetry measurements while at 40K and 370K, sine burst and sine sweep dynamic loading, and acoustic excitation. Materials employed, coupon test data, design and construction, and qualification testing will be discussed.

Introduction

The Microwave Anisotropy Probe (MAP), the first of two selected MIDEX missions, is a follow-on to the successful COBE mission. The COBE mission supported that the model of the universe is not static, but could be better described by an expanding one. This discovery earned Penzias and Wilson the 1978 Nobel Prize in physics, leading to the Big Bang theory. An explosion of such size and temperature to bring the universe into being must have left some mark. The remnant from the Big Bang is the cosmic microwave radiation background, a measurable quantity.

MAP will seek answers to questions about cosmology not answered by COBE. How did structures of galaxies form in the universe? What are the values of the key parameters of the universe? When did the first galaxies form? Why is the cosmic microwave background temperature so uniform on scales > 2°K?

The MAP observatory consists of Dual Back-to-Back Gregorian optics coupled to a Differential Pseudo-Correlation Radiometer operating in the 22 to 90 GHz frequency band. MAP will operate at L2, a location in space with neutral gravity, spin at 70 rpm, and map the entire universe twice during its 26 month mission. Chuck

Bennett of NASA/GSFC is the principal investigator.

On April 1, 1997, Programmed Composites, Inc. was awarded the contract to provide design engineering, fabrication and qualification testing for the Thermal Reflector System (TRS). The TRS consists of 1.4 x 1.6 meter primary mirrors, .80 meter secondary mirrors, dual passive thermal radiators, and a truss structure for mechanical alignment of all components. A schematic of the major components comprising the TRS is shown in the following figure.

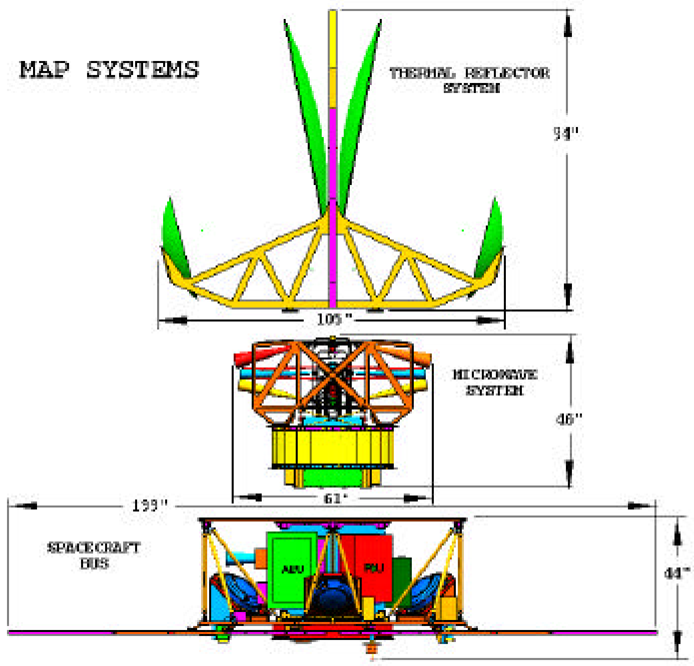

Design Philosophy

At L2, the TRS performs its function while at a generally uniform 50K (-370F). However, fabrication of the composite elements occurs at either 250F or 350F. Final assembly and alignment is done at room temperature. Residual stress between fiber and resin matrix at these differential temperatures can easily lead to warpage and misalignment. Maintenance of critical dimensions between components requires that strict control of Coefficient of Thermal Expansion (CTE) be sustained.

Well known among the spacecraft composites community is the fact that hexagonal honeycomb is orthotropic in nature, and imparts an orthotropic CTE to a otherwise quasi-isotropic CTE sandwich structure. As one example, developed by PCI, is the GeoSat Follow-On spacecraft radiometer, where XN-50A fabric facesheets combined with aluminum honeycomb produced measured CTE's of .35 ppm/F and .45 ppm/F in the plate X and Y directions. For the MAP application, these CTE's are too far from zero, and are not acceptable, but for GFO they are well within established design parameters, since GFO operates in low earth orbit with reflector temperatures near ambient.

Both the primary and secondary reflectors on TRS are of sandwich construction to maximize shell rigidity, and incorporate the higher modulus XN70A spread fabric (75 gm/sq. meter) with DuPont’s Korex honeycomb core. Selection of the Korex was based on uniformity of core construction, reduced CTE and improved strength and stiffness compared to Nomex non-metallic core. The final CTE’s are .03 ppm/F and .15 ppm/F in the reflector X and Y plane.

Supporting rib structure for the reflectors required a matching CTE in the direction along the bonded length with the reflectors. In this case, XN70A tape material together with aluminum core is used. To counteract the forementioned orthotropic nature of the core, a slightly non-quasi-isotropic ply orientation was used, which resulted in final CTE’s of -.02 ppm/F and -.06 ppm/F in the plate X and Y directions. The rib plate X direction is parallel with the reflector surface (bonded edge).

The truss structure supports all components, and attaches to an aluminum ring attached to a gamma-alumina thermal isolation cylinder within the spacecraft body. When integrated with the spacecraft payload, four lift points permit the entire TRS and focal plane assembly to be mated/de-mated from the buss structure. With primary reflectors located high above the interface plane, the dual requirement of high structural stiffness and low CTE led PCI to choose a mortise-tenon design approach. Two styles of corner joints, slotted and nested, are used to form the truss elements. The TRS XZ plane is most critical for dynamic loading during launch. Given our weight, geometric size and configuration limitations, typically, one would incorporate increasingly higher modulus graphite for improvement to the first mode.
However, increasing the fiber modulus causes the CTE to become increasingly more negative. In the TRS YZ plane, the lateral frequency requirements are less stringent, and the primary concern is mechanical load. PCI’s design of the truss, taking in all factors, was to use XN70A/cyanate ester for all faces normal to the XZ plane, and M46J/cyanate ester for all faces normal to the YZ plane. The result is a hybrid truss using two graphite composite materials, each having different stiffness, and with one having positive CTE and the other negative CTE.

Two large radiators are used to remove internal electronic component heat and radiate it to space. These panels employ 1100 series H14 aluminum facesheets and 2 inch thick aluminum core. To save weight, the facesheets were chem-milled in four thickness steps having a pattern equivalent to the heat flow distribution. The two radiators represent over 30% of the total TRS weight.

Materials Employed

The PCI approach to the TRS design was to manage the thermal deformations through materials selection and fiber orientation, manage the overall stiffness through shape control of elements and stiffeners, and overall weight control through optimization of detail parts.

The list of materials used on the TRS is shown in Table 1.

TRS Materials Selection and Properties

	Layup	Modulus		Tension Strength		CTE (ppm per F)		CME (ppm per %M)	
Primary/Secondary Reflector Shells		Longitudinal	Transverse	Longitudinal	Transverse	Longitudinal	Transverse	Longitudinal	Transverse
Nippon SF-70A-75 Spread Fabric/YLA RS-12D Re	[0/45/45/0]s	14.05 msi	13.90 msi	47540 psi	47600 psi	0.03	0.15	1	12
DuPont Korex Aramid Honeycomb Core									
Cytec FM 73M Film Adhesive									
Primary Reflector Ribs									
Nippon XN70A Uni Tape/YLA RS-3 Resin	[0/±49/90/90/±49/0]s	19.85 msi	23.87 msi	42200 psi	50420 psi	-0.06	-0.02	18	0
Hexcel 1/8-5056-.007 3.1 PCF Aluminum Core									
Cytec FM 73 Reticulated Film Adhesive									
Secondary Reflector Ribs and Hat Ring									
Toray M46J Uni Tape/YLA RS-3 Resin	[0/45/90/-45]s	12.30 msi	12.1 msi	92900 psi		0.13	0.14	62	N/A
Truss YZ Lateral Plane Truss Elements									
Toray M46J Uni Tape/YLA RS-3 Resin	[0/45/90/-45]s	12.30 msi	12.1 msi	92900 psi		0.13	0.14	62	N/A
Truss XZ Longitudinal Plane Truss Elements									
Nippon XN70A Uni Tape/YLA RS-3 Resin	[0/0/±45/90/0/0/90/±45/0/0]s	32.9 msi	N/A	110000 psi		-0.21	N/A	67	0
Radiators									
1100 H14 Series Pure Aluminum Sheet (Chem Milled)		9.9 msi	9.9 msi	6000 (Endurance Limit)		11.9	11.9	0	0
Hexcel 3/8-5056-.0007 1.0 PCF Aluminum Core									
Cytec FM 73 Reticulated Adhesive									

Design Details

The TRS design is composed of four major sub-assemblies. Primary reflectors, secondary reflectors, truss structure, and radiators.

Primary reflector shape is determined from a software package furnished by Princeton. Given a local x-y coordinate, the program generates the local z, resulting in a shaped surface having no unique focal point. From points generated over a .50 inch square grid, a surface was created using SDRC's Ideas software. Accuracy of the generated surface to the theoretical was checked at all locations, and was found to be within 5E-5 inches. One tool was created for the primary reflector, and another for the secondary. Two quasi-isotropic facesheets, balanced and mirrored from the prepreg stock were fabricated. The core is bonded while the cured facesheet is held to the tool with vacuum. Subsequently, the core is machined to the same shape as the tool, but offset. Finally, the rear facesheet is bonded to the core.

The purpose of this design/manufacturing approach is to negate any mechanical stresses conceivably imparted by the manufacturing processes. Core bonding occurs at the stress free temperature of the facesheets. In spite of our best efforts to mitigate reflector warpage at its operational temperature, a temperature differential of –356C (–640F) from the bonding temperature, the unsupported outboard reflector edges elastically deformed beyond specification, and a hat shaped stiffener was subsequently added. The secondary reflectors followed an identical design/manufacturing path. There also, a hoop ring/radial rib structure was added to mitigate the operational thermal deformations.

The truss structure presented some interesting challenges. The TRS interface to the MAP structure is to the upper surface of a gamm-alumina cylinder having an aluminum T shaped ring. The TRS is bolted to this T ring. At 70K, the ring shrinks .080 inches radially, which the PCI truss needed to accommodate. The design approach selected is the use of four I beam shaped Titanium flexures. Being a hard interface, all axial loads and bending moments are carried through the flexures at launch, while still retaining sufficient flexibility to accommodate relative displacements when at L2.

A mortise-tenon design approach for the truss was selected due to thermal deformation concerns and the need to establish high structural rigidity. At the beginning, PCI considered about 15 truss configuration possibilities. A popular choice is to fabricate square tubes, and join them using bonded gussets and clips. Using multiple tooling, layups and cure cycles, our fear was that all tubes would not be identical, leading to grading, CTE measurement and selection from multiple candidates. Similarly, other competitive design approaches were discarded due to uncertainties and manufacturing cost risk.

Ultimately, the mortise-tenon approach allowed PCI to fabricate one very large flat sheet of material, and CNC machine the truss elements in a very predictable manner. This approach also allowed the use of two complementary materials and fiber orientations to solve the CTE and stiffness issues. Any truss element face parallel to the XZ plane is quasi-isotropic M46J/RS3 with a slightly positive CTE, while any truss element face parallel to YZ plane is XN70A/RS3 with a slightly negative CTE. The XN70 faces are not quasi-isotropic, but a layup maximizing in-plane stiffness within the allowable CTE range. This methodology is commonly referred to as “athermalizing”. A break-away view of the truss is shown below.

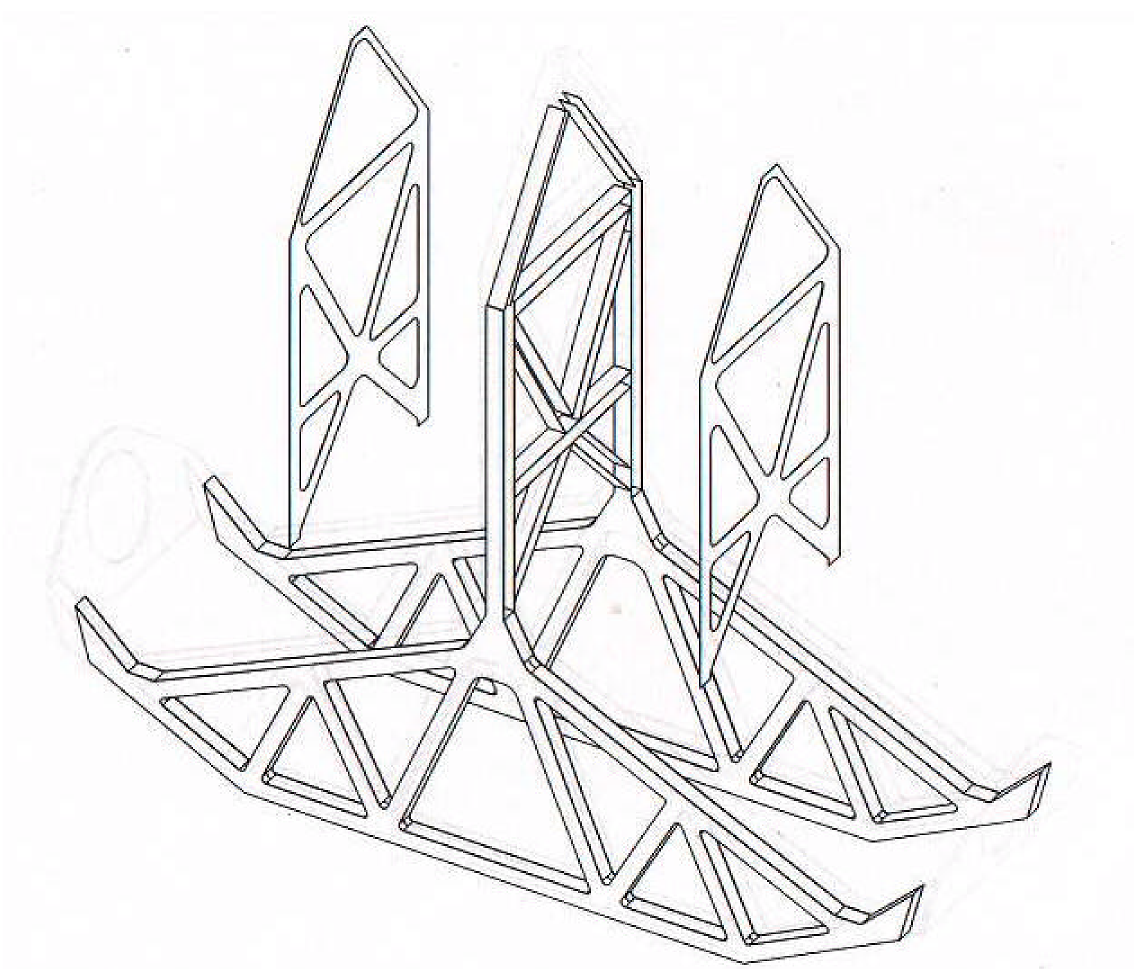

Radiators are employed to maximize the efficiency of the Low Noise Amplifiers at the feed horns. These large panels are fabricated using Series 1100 H14 pure aluminum for the facesheets and standard honeycomb core. To achieve the weight budget, including the radiators, PCI selectively chem-milled the facesheets in four steps based on heat flow contour plots provided by Goddard. At all load/support points, the .090 inch thickness was retained, with .063, .040 and .020 thickness in the outboard regions. A design requirement was to thermally isolate the radiators from the remaining structure. The lower support point uses G-10 flat stock as fitting tabs, aluminum lateral support tubes use G-10 fitting inserts, and the upper support flexure is a folded back Titanium sheet stock design. A maximum allowable .75 watts heat leak requirement was met analytically and experimentally verified.

The main features of the TRS design, and a number of the details are found in the isometric view shown below.

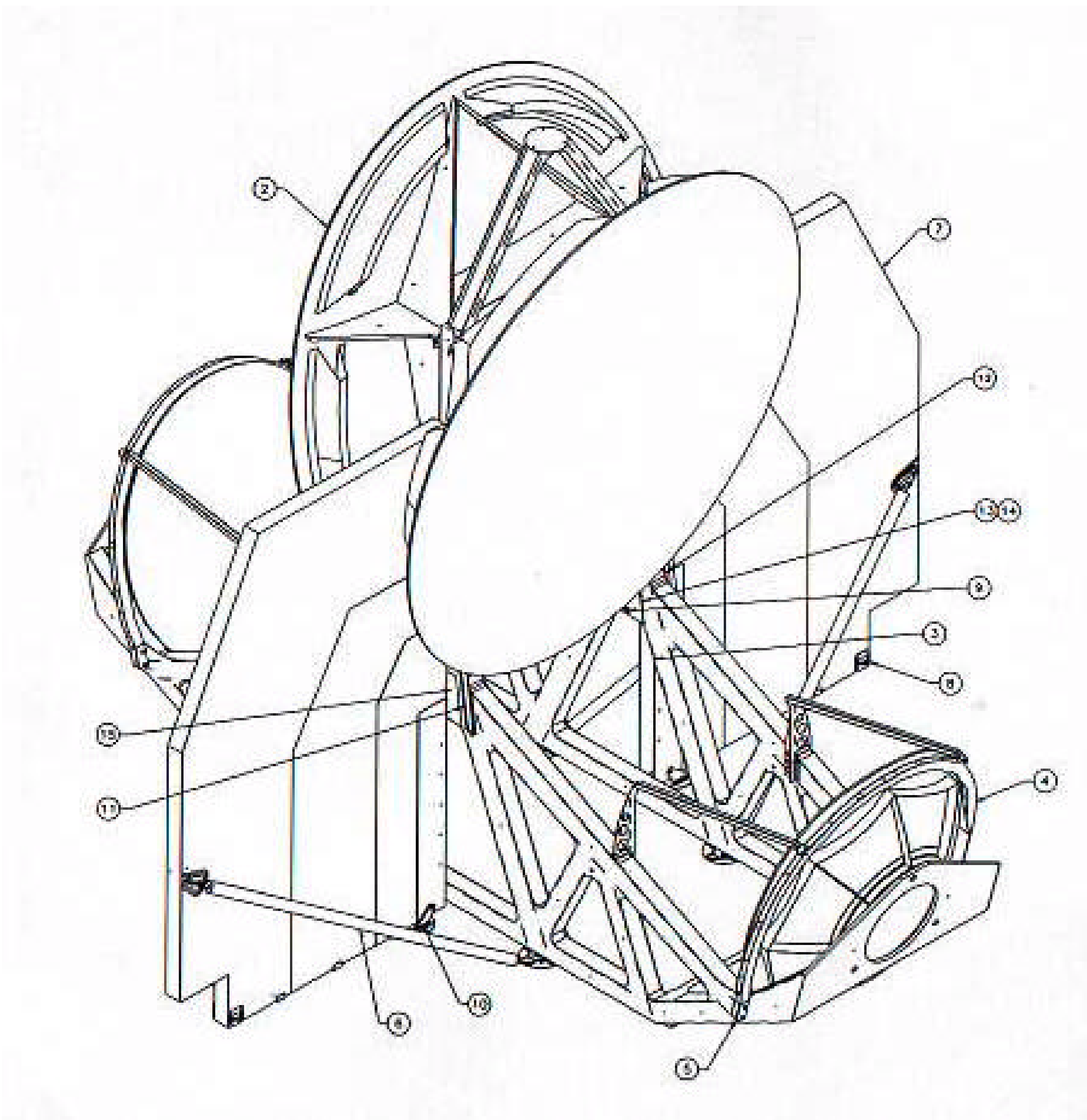

Mechanical Testing

The TRS assembly has been subjected to these tests, representing all major phases of flight and data collection.

- Hot Soak to 100C (Vacuum)
- Cold Soak to 40K (Vacuum)
- Sine Burst (Ambient)
- Sine Sweep (Ambient)
- Acoustic Excitation (Ambient)

Hot Soak Test

The hot soak test was performed to simulate solar heating effects during the 'barbecue' roll mode during earth-moon phasing loops. This test also provides the data to calculate a Cold Thermal Time Constant, provide model correlation for one steady state sun on the primary reflector, and support Bi-Reflectance Distribution Function test results. Although the time at peak temperature (100C) is a relatively short 10 minutes, concern was for visco-elastic realignment of the reflectors. At 100C, the film adhesive used in the sandwich is at its glass transition temperature.

A large bank of heating lamps was assembled at Goddard, and temperatures were monitored so that the time-temperature profile would not be exceeded. Displacement measurement of the truss, primary and secondary reflectors, and the radiators was carried out using photogrammetry. The TRS met all requirements, and no permanent deformation or realignment of the structure was measured.

Cold Soak Test

The cold soak test represents the simulation of temperature while in data collection mode at L2. A large vacuum chamber at Goddard was used, with LHe as the cooling medium within the shroud. Within the chamber, a rotating gantry assembly held the photogrammetry equipment, used to validate the surface accuracy and alignment of the entire TRS. As a result of this test, the addition of the hat stiffeners at the perimeter of the primary reflectors was deemed necessary. The 'sweet spot' of the both primary and secondary reflectors were shown to meet specification of .0015 inches rms when at this steady cold condition (40K). A subsequent test at LN2 temperatures proved the surface accuracy requirements had been met. A supplemental requirement at the 40K condition was that no point anywhere on the TRS could deviate outside a .020 inch positional location.Subsequent to the cold testing, extensive visual inspection was performed. There were no anomalies of any kind found.

Acoustic Test

Goddard has a very large acoustic chamber. Upon completion of the vibration test sequence, two acoustic runs were performed (-6db and protoflight). Test duration is 60 seconds for both levels. It is interesting to be standing outside the chamber with the large steel doors closed. The impression is that one is at the launch pad.

This test was uneventful except one accelerometer became debonded. A photo of the TRS and test personnel illustrates the size of the chamber.

The TRS is a stiff structure, and therefore, acoustic loading was not expected to excite large accelerations. RMS accelerations and forces from the test are captured in the following table.

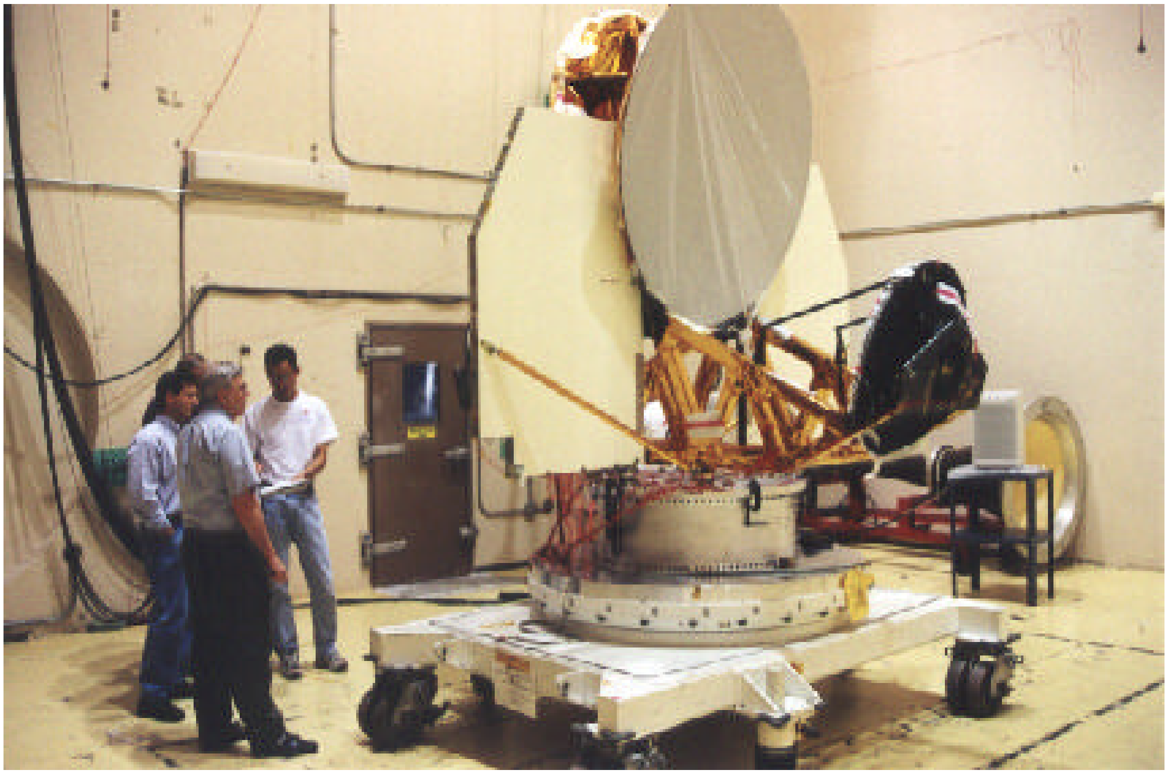

Table 3 RMS Accelerations and Forces

Location Number	Type	Location Description	X (g_{rms} or $\#_{rms}$)	Y (g_{rms} or $\#_{rms}$)	Z (g_{rms} or $\#_{rms}$)
1	Accelerometer	+X truss outer face at +Y secondary reflector	23.92	(N/A)	(N/A)
2	Accelerometer	-X truss outer face at +Y secondary reflector	24.73	(N/A)	(N/A)
3	Accelerometer	-X truss outer face at -Y secondary reflector	23.76	(N/A)	(N/A)
4	Accelerometer	+X truss outer face at -Y secondary reflector	19.56	(N/A)	(N/A)
5	Accelerometer	Omni	5.33	23.28	4.43
6	Accelerometer	+Y secondary reflector back	4.92	15.11	13.04
10	Accelerometer	-Y secondary reflector back	5.84	15.57	9.93
7	Accelerometer	+X radiator strut fitting on radiator	(N/A)	17.45	(N/A)
11	Accelerometer	-X radiator strut fitting on radiator	(N/A)	16.81	(N/A)
8	Accelerometer	+Y primary reflector +X upper rib edge	3.74	11.91	18.17
9	Accelerometer	+Y primary reflector -X upper rib edge	3.75	11.89	17.25
12	Accelerometer	-Y primary reflector +X upper rib edge	2.88	11.39	17.37
13	Accelerometer	-Y primary reflector -X upper rib edge	(N/A)	(N/A)	(N/A)
14	Accelerometer	+X truss apex	3.72	4.05	(N/A)
15	Accelerometer	-X truss apex	3.93	4.55	(N/A)
16	Accelerometer	+X radiator upper outer edge	(N/A)	34.28	(N/A)
18	Accelerometer	-X radiator upper outer edge	(N/A)	35.84	(N/A)
17	Accelerometer	-X radiator flexure	11.74	10.38	30.70
19	Accelerometer	+X radiator flexure	10.79	11.67	32.72
201	Force gauge	+X+Y I/F flexure / radiator strut	39.21	27.42	175.13
202	Force gauge	-X+Y I/F flexure / radiator strut	42.33	32.06	89.06
203	Force gauge	-X-Y I/F flexure / radiator strut	41.92	29.06	126.94
204	Force gauge	+X-Y I/F flexure / radiator strut	44.79	33.15	120.84
211	Force gauge	+X lateral strut / radiator	12.41	29.89	30.73
212	Force gauge	-X lateral strut / radiator	12.78	29.88	206.95 (*)

* PSD from this channel did not look correct; loose cable suspected.

Sine Burst/Sine Sweep Tests

Sine burst and sine sweep testing were performed at Goddard. The TRS was instrumented with 19 accelerometers and 6 force gages, as shown in the following table.

In terms of strength qualification, the environment during the sine burst test is more severe than during the sine sweep

Table 2 Instrumentation

Location Number	Number of Channels	Degrees of Freedom	Type	Location Description
1	1	X	Accelerometer	+X truss outer face at +Y secondary reflector
2	1	X	Accelerometer	-X truss outer face at +Y secondary reflector
3	1	X	Accelerometer	-X truss outer face at -Y secondary reflector
4	1	X	Accelerometer	+X truss outer face at -Y secondary reflector
5	3	X Y Z	Accelerometer	Omni
6	3	X Y Z	Accelerometer	+Y secondary reflector back
7	1	Y	Accelerometer	+X radiator strut fitting on radiator
8	3	X Y Z	Accelerometer	+Y primary reflector +X upper rib edge
9	3	X Y Z	Accelerometer	+Y primary reflector -X upper rib edge
10	3	X Y Z	Accelerometer	-Y secondary reflector back
11	1	Y	Accelerometer	-X radiator strut fitting on radiator
12	3	X Y Z	Accelerometer	-Y primary reflector +X upper rib edge
13	3	X Y Z	Accelerometer	-Y primary reflector -X upper rib edge
14	2	X Y	Accelerometer	+X truss apex
15	2	X Y	Accelerometer	-X truss apex
16	1	Y	Accelerometer	+X radiator upper outer edge
17	3	X Y Z	Accelerometer	-X radiator flexure
18	1	Y	Accelerometer	-X radiator upper outer edge
19	3	X Y Z	Accelerometer	+X radiator flexure
201	3	X Y Z	Force gauge	+X+Y I/F flexure / radiator strut
202	3	X Y Z	Force gauge	-X+Y I/F flexure / radiator strut
203	3	X Y Z	Force gauge	-X-Y I/F flexure / radiator strut
204	3	X Y Z	Force gauge	+X-Y I/F flexure / radiator strut
211	3	X Y Z	Force gauge	+X lateral strut / radiator
212	3	X Y Z	Force gauge	-X lateral strut / radiator

vibrations. The levels were derived from coupled loads analysis, which involved integrating the TRS model with other instrument and spacecraft models to a form a full-up MAP observatory model. Loads from the Delta 7425-10 launch vehicle flight environment were applied to this model, with force and acceleration outputs captured throughout the TRS.

The levels are different in each axis. Using axis dependent loads was justified since the TRS load paths depend on load direction. Loading in the Y-axis qualified the interface flexures, radiator flexures and strut connections. The X-axis burst qualified the lateral strut/radiators. The Z-axis qualified the overall configuration at lift-off.

A picture of the TRS while on the shaker provides some insight of the setup.

The typical test sequence consisted of a low level sine sweep from 5 to 50 Hz at 4 octaves/minute. Then, sine burst testing was initiated at –6db and –3db levels, with the final run level increased to reach the required accelerations. A low level sine sweep was performed between each burst level. A final sine sweep at full level, followed by a low level completed the vibration sequence. This was done in each axis. These tests produced voluminous output data. A typical summary of the force gage output is seen in the table.

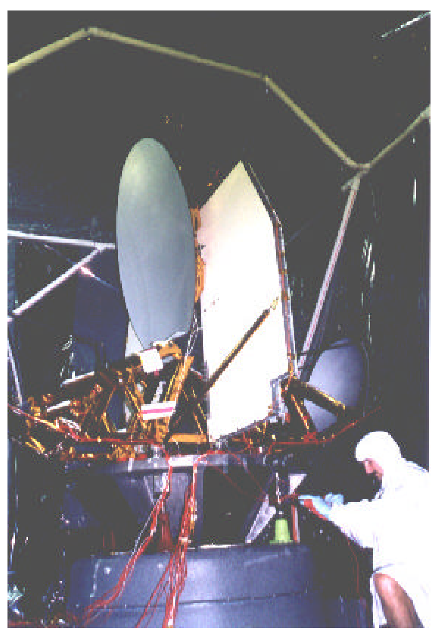

Table 4 Force Gauge Measurements for Y-axis Sine Burst, 14.0 g (-6 dB) at 20 Hz

I/F Flexures / Radiator Struts

		FX (#)	FY (#)	$[FX^2 + FY^2]^{1/2}$ (#)	FZ (#)
Analytical (*)		511.0	431.2	668.6	953.4
		(375.5)	(289.7)	(474.3)	(899.4)
		FX (#)	**FY (#)**	**$[FX^2 + FY^2]^{1/2}$ (#)**	**FZ (#)**
Test	FG 201	+510.9 / -446.2	+371.8 / -409.4	654.7	+1641.2 / -1852.5
	FG 202	+492.2 / -442.9	+392.4 / -371.8	629.5	+1212.5 / -1297.3
	FG 203	+454.6 / -546.4	+396.1 / -375.4	674.9	+1243.1 / -1286.2
	FG 204	+483.2 / -486.1	+358.4 / -393.5	625.4	+1268.3 / -1231.7
		FX ratio	**FY ratio**	**$[FX^2 + FY^2]^{1/2}$ ratio**	
Ratio of Test Over Analytical	FG 201	1.00	0.95	0.98	
	FG 202	0.96	0.91	0.94	
	FG 203	1.07	0.92	1.01	
	FG 204	0.95	0.91	0.94	

Lateral Struts / Radiators

		FX (#)	FY (#)	$[FX^2 + FY^2]^{1/2}$ (#)	FZ (#)
Analytical (*)		0.0	109.3	109.3	0.0
		(68.1)	(16.7)	(70.1)	(548.5)
		FX (#)	**FY (#)**	**$[FX^2 + FY^2]^{1/2}$ (#)**	**FZ (#)**
Test	FG 211	+46.8 / -48.4	+107.6 / -109.7	119.9	+134.3 / -141.5
	FG 212	+33.7 / -49.3	+119.0 / -120.3	130.0	+111.9 / -95.6
			FY ratio		
Ratio of Test Over Analytical	FG 211		1.00		
	FG 212		1.10		

TRS test item weight (#) 146.0

Force sum Σ Y (#) +1724.1 / -1703.6

Shear based net CG acceleration (g) +11.81 / -11.67

* Forces on first row are from 14.0 g +Y applied to a stand-alone, fixed-base TRS NASTRAN model.
Forces in parentheses are 1.1 * CLAI3 results.

Summary of Testing

The TRS has been subjected to tests simulating all phases of flight, and has been deemed suitable for integration to the MAP structure. As a consequence of these tests, minor changes to the design were required, which were incorporated by PCI while the structure was at NASA/Goddard. A triangular stiffener was necessary at the junction of the truss apex and the primary reflectors to increase a Y axis mode. Mechanical fasteners were added to the brackets supporting the lateral struts, elevating peel stress concerns at the attachment bracket. Subcomponent tests confirmed fatigue strength of the G-10 radiator supports, flexure buckling strength, and flexure housing static ultimate strength.

PCI expects the TRS to perform its intended function during its mission lifetime, and perform its function in providing answers to the origins of the universe.